



Sensitivity of mixed-phase moderately deep convective clouds to parameterisations of ice formation - An ensemble perspective

Annette K. Miltenberger¹ and Paul R. Field^{2,3}

¹Institute for Atmospheric Physics, Johannes Gutenberg-University, Mainz, Germany

²Institute of Climate and Atmospheric Science, School of Earth and Environment, University of Leeds, United Kingdom

³Met Office, Exeter, United Kingdom

Correspondence: Annette K. Miltenberger (amiltenb@uni-mainz.de)

Abstract. The formation of ice in clouds is an important processes in mixed-phase and ice-phase clouds. Yet, the representation of ice formation in numerical models is highly uncertain. In the last decade several new parameterisations for heterogeneous freezing have been proposed. It is so far unclear what the effect of choosing one parameterisation over another is in the context of numerical weather prediction. We conducted high-resolution simulations ($\Delta x = 250\text{m}$) of moderately deep convective clouds (cloud top $\sim -18^\circ\text{C}$) over the southwestern UK using several formulations of ice formation and compare the resulting changes in cloud field properties to the spread of an initial condition ensemble for the same case.

The strongest impact of altering the ice formation representation is found in the hydrometeor number concentration and mass mixing ratio profiles. While change in accumulated precipitation are around 10 %, high precipitation rates (95th percentile) vary by 20 %. Using different ice formation representations changes the outgoing short-wave radiation by about 2.9 W m^{-2} averaged over daylight hours. The choice of a particular representation for ice formation has always a smaller impact than omitting heterogeneous ice formation completely. Excluding the representation of the Hallett-Mossop process or altering the heterogeneous freezing parameterisation has an impact of similar magnitude on most cloud macro- and microphysical variables with the exception of the frozen hydrometeor mass mixing ratios and number concentrations.

A comparison to the spread of cloud properties in a 10-member high-resolution initial condition ensemble shows that the sensitivity of hydrometeor profiles to the formulation of ice formation processes is larger than sensitivity to initial conditions. In particular, excluding the Hallett-Mossop representation results in profiles clearly different from any in the ensemble. In contrast, the ensemble spread clearly exceeds the changes introduced by using different ice formation representations in accumulated precipitation, precipitation rates, condensed water path, cloud fraction and outgoing radiation fluxes.



1 Introduction

Clouds consisting of a mixture of liquid and solid particles (mixed-phase) clouds play an important role for weather and climate at all latitudes. For example, observational data suggest that a significant fraction of surface precipitation form in mixed-phase clouds (e.g. Field and Heymsfield, 2015). It has also been demonstrated that the representation of cloud glaciation in global climate models has a substantial impact on the simulated mean climate state (e.g. McCoy et al., 2016). Despite this importance of mixed-phase clouds, for predicting weather and climate, the physical understanding of the underlying processes, most importantly ice formation, is very limited. Not surprisingly the representation of mixed-phase is one key source of uncertainty in weather and climate models (e.g. Korolev et al., 2017).

The formation of ice particles in the atmosphere has received particular attention over the last decades. Although the underlying physics of ice nucleation are still not understood, data from laboratory and field measurements has been used to suggest a number of new parameterisations that relate the aerosol population and environmental temperature to the number of nucleating ice crystals (e.g. DeMott et al., 2010, 2015; Niemand et al., 2012; Atkinson et al., 2013; Wilson et al., 2015). These new formulations gradually replace older formulations used in numerical weather prediction models (e.g. Cooper, 1986; Meyers et al., 1992). While it has been demonstrated that more sophisticated formulations of heterogeneous freezing, in particular its dependency on the aerosol population, is beneficial for predicting certain cloud types (e.g. Klein et al., 2009; Vergara-Temprado et al., 2018), it is not clear what the impact of choosing one parameterisation over another parameterisation is. A recent publication by Hawker et al. (2020) suggests that the increase of ice nucleating particle number concentration per unit decrease of temperature, i.e. the slope of the parameterisation, plays a key role in determining the impact of a specific parameterisation on the simulated tropical deep convective cloud field.

In addition to heterogeneous and homogeneous freezing of solution droplets, new ice particles can also be formed by so-called secondary ice formation processes, of which the Hallett-Mossop process is the most well known (e.g. Field et al., 2017). Although secondary ice formation seems to be crucial to explain observed ice crystal number concentration in many clouds, its representation in numerical models is highly uncertain and its importance for determining cloud properties is still debated (e.g. Field et al., 2017). Formulations for processes other than the Hallett-Mossop processes have only become available recently (e.g. Sullivan et al., 2018).

Here, we investigate the impact of using different heterogeneous freezing parameterisation and including a representation of the Hallett-Mossop process on the simulated evolution of moderately deep convective clouds (cloud top temperature around -18°C) over the United Kingdom. Thereby we expand the study by Hawker et al. (2020) to a different cloud regime.

The standard approach to estimate the impact of altered cloud microphysical parameterisations is to conduct sensitivity experiments. The differences between the various experiments are interpreted as the impact of the parameterisation change. To assess the importance of the identified sensitivity in the context of model development and improvements for numerical weather prediction, it is, however, vital to compare the sensitivity to changes in one parameterisation to the uncertainty of the prediction due to other deficiencies in the model formulation and the overall predictability of the considered case. The latter is in particular important for convective situations with a small intrinsic predictability, as in these conditions any small



perturbation may rapidly amplify (e.g. Hohenegger and Schär, 2007; Dey et al., 2014). The relevance of taking into account the predictability of different situations for assessing the sensitivity to parameterisation changes is gaining increasing attention (e.g. Wang et al., 2012; Posselt et al., 2019). Quantifying the relative importance of initial condition uncertainty and uncertainty due to the model formulation is important for identifying priorities in future model development and justifying investment in more complex model formulations for operational weather forecasting centres. To address this issue, we place the sensitivity experiments in the context of a high-resolution initial condition ensemble.

The two key research questions addressed in the paper are:

- How sensitive are mixed-phase convective clouds with cloud top temperatures around -18°C to the parameterisation of ice formation (heterogeneous freezing and Hallett-Mossop process)?
- How does the sensitivity to different descriptions of ice formation compare to typical initial condition uncertainty for day-1 forecasts?

The paper starts with a short introduction to the investigated case and the model framework used for the simulations (section 2). The results from the sensitivity experiments are presented in section 3 and place them in the context of the ensemble simulations in section 4. Finally, the key findings are summarised and discussed in section 5.

2 Model and data

Simulations were conducted for the 3rd August 2013 case from the COPE campaign Blyth et al. (2015); Leon et al. (2016); Miltenberger et al. (2018a). The campaign took place over the Southwestern Peninsula of the British Isles and probed convective clouds forming along converging sea-breeze fronts. We use the Unified Model vn10.3 with the Cloud Aerosol Interacting Microphysics Module (CASIM). The model set-up is identical to that described in Miltenberger et al. (2018a, b). A regional nest with a grid spacing of 1 km resolution is nested in the global simulations, which in turn drives a second nest with a grid spacing of 250 m. Only data from the innermost nest is used here. The initial and lateral boundary conditions for the 1 km nest are derived from the operational control run and nine members of the global operational ensemble forecast from the Met Office (MOGREPS, Bowler et al. (2008)), which represent the anticipated spread of moisture and moist energy convergence over the region of interest (see also Miltenberger et al. (2018b)). The aerosol environment is represented by using a constant profile for initial and boundary conditions, which has been derived from aircraft observation (“standard” aerosol scenario in Miltenberger et al. (2018a)), and by allowing for advection of aerosols in the domain. Aerosol properties influence cloud droplet and ice crystal formation, but the cloud microphysical processes do not alter the aerosol properties (“passive” mode in Miltenberger et al. (2018a)). Further detail on the model set-up and the cloud microphysics parameterisation can be found in Miltenberger et al. (2018a).

Substantial parametric and systematic structural uncertainty resides in the model representation of cloud microphysical processes, in particular with regard to ice formation processes. Several heterogeneous freezing parameterisations, which differ in the used parameters and the form of the temperature dependence of ice formation (e.g. Hawker et al., 2020), have been



suggested over the last decade. In order to investigate the implications of choosing specific schemes for numerical weather prediction, a set of new simulations has been conducted: seven simulations with different heterogeneous freezing parameterisation (“FSENS”), one simulation omitting the parameterisation of the Hallett-Mossop process (“NoHM”), and one omitting all ice-phase processes (“WARM”). For the FSENS experiments we used the heterogeneous freezing parameterisations by Meyers et al. (1992) (M92), Atkinson et al. (2013) (A13), DeMott et al. (2010) (DM10), DeMott et al. (2015) (DM15), Niemand et al. (2012) (N12), and Tobo et al. (2013) (T13). The DM10 parameterisation is used in the “NoHM” simulation. In addition, two simulations with pre-factors of 10 and 0.1 for the DM10 parameterisation are included, which represent high- and low-INP regimes. The simulation with the DM10 parameterisation is identical to the the “control” simulation in Miltenberger et al. (2018b) and is referred to as “baseline” simulation in the following. Initial and lateral boundary conditions for these sensitivity experiments are derived from the operational global control run.

The control run with the DM10 parameterisation has been compared to observational data in Miltenberger et al. (2018a), where we could demonstrate that it successfully captures many features of the observed cloud and precipitation evolution, the thermodynamic conditions and cloud microphysical parameters. Hence the set-up provides a meaningful framework for the sensitivity analysis presented here.

3 Sensitivity of cloud field properties to representation of ice formation

Varying the representation of primary and/or secondary ice formation has a direct impact on the number of ice crystals produced at a specific temperature, and hence ice crystal number concentrations (ICNC) vary between the different experiments. Despite a multitude of other processes altering ICNC in a complex cloud field, systematic variations in the average ICNC profile appear in the different experiments (Fig. 1 c). The profiles used here are average in-cloud profiles over the time period 10 UTC to 19 UTC. Differences are largest towards cloud top, with a spread of about one order of magnitude at 5 km altitude. Cloud bases are located roughly at 1 km altitude, cloud tops are located at 5.5 – 6 km altitude and the 0 °C level is found at around 2.6 km altitude (Miltenberger et al., 2018a). In the altitude range, where the Hallett-Mossop processes is active (i.e. 3 – 4 km altitude corresponding to roughly –3 to –8 °C), ICNC concentrations vary by about a factor 2 between the FSENS experiments, while ICNC concentrations in the NoHM run are about 1.5 orders of magnitude smaller than in any FSENS experiment. Despite this clear signal of the Hallett-Mossop process in the 3 – 4 km altitude range, ICNC towards cloud top reaches similar values as in the FSENS experiments.

The differences in ICNC can impact the occurrence of other hydrometeor species via various cloud microphysical processes (Fig. 1): Snow crystal concentrations vary by up to a factor 2 between the different FSENS experiments and it is by a factor 5 lower in the NoHM experiment. In contrast to the signal in ICNC, the imprint of the Hallett-Mossop processes is consistent throughout the cloud layer. Interestingly, the variation in graupel number concentration is largest of all frozen hydrometeor types. Again the NoHM simulation displays the lowest number concentration. Altering the representation of ice formation also impacts the number concentration of liquid hydrometeors, particularly in the upper cloud parts: While the cloud droplet number concentration (CDNC) in the WARM simulation is almost constant with altitude, CDNC is significantly reduced in the



FSENS and NoHM experiments above about 3 km. This is likely a consequence of freezing and collection by ice, snow and graupel particles. Interestingly, FSENS experiments with a high ICNC above 5 km have a low CDNC and vice-versa, implying a major impact of cloud droplet freezing. Variations in rain number concentrations are somewhat smaller than in CDNC. The profiles from the NoHM experiment feature roughly in the middle of the FSENS experiments for both cloud droplet and rain drop number concentration, i.e. the main impact of the Hallett-Mossop process is limited to frozen hydrometeor species in our simulations. If instead of the mean number concentration the 95th percentile is considered, the general behaviour is very similar to that just discussed for the mean profiles (SI Fig. 1). The one outstanding difference is a much larger ice crystal number concentration in the simulation with enhanced INP concentrations (“HighDM”). This suggests that while higher INP concentrations result in an enhanced ice crystal formation, as is to be expected, the impact on mean ice crystal number concentration is much smaller due to the depletion of ice crystals by other microphysical processes, such as for example conversion to snow or graupel.

The average profiles of hydrometeor mass mixing ratios essentially mimic the sensitivities just discussed for the hydrometeor number concentrations (Fig. 2). Ice, snow and graupel mass mixing ratios are consistently lower in the NoHM experiment than in all other experiments. Differences in ice, cloud droplet and rain drop mass mixing ratios occur mainly in the upper part of the clouds (above ~ 3.5 km), while variation in snow (graupel) mass mixing ratio are small (large) throughout the entire cloud layer.

Different representations of ice formation clearly impact the cloud microphysical structure of the moderately deep convective clouds from COPE. We now investigate how these changes impact larger-scale features of the cloud field, such as accumulated precipitation and top-of-the-atmosphere radiation fluxes. Accumulated surface precipitation varies by about 8 % between FSENS experiments (Fig. 3 a). While omitting secondary ice formation leads to an increase in accumulated precipitation of about ~ 6 % relative to the baseline simulation, omitting all ice formation results in a reduction of accumulated precipitation by about ~ 21 %. It is not straightforward to understand the changes in accumulated precipitation from the differences in the cloud microphysical composition of the clouds. Therefore, we choose to investigate the cloud condensate budget as suggested for example by Khain (2009) and Miltenberger et al. (2018a). Differences in accumulated condensate generation G and condensate loss L are calculated relative to the baseline simulation, i.e. using DM10. In the scatterplot of ΔG against ΔL FSENS and NoHM experiments cluster on the one-to-one line (Fig. 4 a). Relative changes in G and L are ≤ 2 % for FSENS experiments. In the NoHM experiments changes to G and L are larger (~ 4 %), but balance each other resulting in a small net change in accumulated precipitation. Combined with the much larger changes in the cloud microphysical structure, this implies that changes in precipitation formation via a specific cloud microphysical pathways are compensated by changes in other pathways resulting in an overall similar integrated precipitation production. The only experiment displaying a different behaviour is the WARM experiment: While condensate generation decreases by ~ 5 %, condensate loss only decreases by ~ 0.1 %. The reduction in accumulated precipitation compared to the baseline simulation is hence the result of much less condensate being produced in the WARM experiment. If assuming the vertical displacement of parcels does not change between simulations and any produced supersaturation is depleted by condensate formation, this is consistent with the lower saturation vapour pressure over ice than over water. However, without supporting evidence this remains a hypothesis. Further, a negative



ΔG and no change in ΔL implies that the precipitation efficiency in the WARM experiment is larger than in any experiment with ice microphysics. Precipitation efficiency is defined here as the ratio of time- and domain-integrated precipitation rate to condensation and deposition rate. This response is contrary to what has been reported for isolated orographic clouds (e.g. Barstad et al., 2007; Miltenberger, 2014) and the larger precipitation efficiency for more rapidly glaciating clouds in high-INP environments found in global climate model simulations (e.g. Lohmann and Hoose, 2009). However, a reduction in precipitation efficiency with an increased cloud glaciation has been also found by Levin et al. (2005) for convective clouds in the Mediterranean.

Similar to the accumulated precipitation, the precipitation rate distribution displays only a weak sensitivity to the parameterisation used for the representation of primary ice formation (Fig. 3 b). Again, the only experiment with a substantially different behaviour is the WARM experiment, which displays a shift towards more intense precipitation: High precipitation rates ($\geq 20 \text{ mm h}^{-1}$) are more frequent, while medium rain rates between 1 mm h^{-1} and 10 mm h^{-1} are about 10 % less frequently. Very high precipitation rates, i.e. the 95th and 99th percentile, display the largest changes. The 95th percentile varies by about 20 % between FSENS experiments and increases by 50 % in the WARM experiment compared to the mean of the FSENS experiments (SI Fig. 2).

The condensed water path and the cloud fraction are other important properties of the cloud field. The difference in the condensed water path between FSENS and NoHM experiments is 29 % of the water path in the baseline simulation ($(CWP(t)_{\max} - CWP(t)_{\min})/CWP(t)_{\text{baseline}}$) in the late afternoon ($\sim 15 - 17 \text{ UTC}$), but smaller values prevail at other times resulting in an average maximum spread between FSENS and NoHM experiments of 14 % (Fig. 5 a). In the WARM experiment the condensed water path is lower than in any other experiment throughout most of the afternoon (maximum: 41 %, mean: 16 % reduction compared to the baseline experiment). This is consistent with the smaller condensate generation and enhanced precipitation efficiency diagnosed for this experiment. Changes in cloud fraction between the different experiments amount at maximum to 20 % of the value in the baseline experiment (Fig. 5 b). Cloud fraction is defined as the areal fraction of the domain with column-integrated condensed water path larger than 1 g m^{-2} . Again, the maximum differences occur in the late afternoon hours. Averaged over the entire time-period, the changes are much smaller (7%).

Finally, we also consider the sensitivity of outgoing shortwave and longwave radiation (Fig. 6). The maximum domain mean difference between any two FSENS/NoHM experiments is about 6 W m^{-2} for the shortwave component and 0.5 W m^{-2} for the longwave component. The average over the considered time-period amounts to 2.9 W m^{-2} (0.27 W m^{-2}) for the shortwave (longwave) component. Similar to the other cloud field characteristics discussed so-far the largest change occurs in the WARM experiment with a maximum (average) increase of 15 W m^{-2} (5.7 W m^{-2}) in the shortwave component and a maximum (average) decrease of 1.4 W m^{-2} (0.5 W m^{-2}) in the longwave component.

Considering the temporal evolution of most cloud properties, i.e. domain-integrated precipitation (not shown), condensed water path (Fig. 5 b) and top-of-the-atmosphere outgoing radiation (Fig. 6), the consistency in the evolution between different experiments is noteworthy, which strongly suggests that the COPE clouds are strongly dynamically forced with little leeway for cloud microphysics to change the overall characteristics of the cloud field.

Overall the sensitivity to the representation of ice formation found here for moderately deep convective clouds (cloud top



195 $\sim -18\text{ }^\circ\text{C}$) is smaller than reported for tropical deep convective clouds (e.g. Hawker et al., 2020). Hawker et al. (2020) find differences of up to 21 W m^{-2} in the total outgoing radiation in a set of simulations comparable to our FSENS experiments. The majority of the signal reported in Hawker et al. (2020) is due to changes in anvil properties. This likely explains the smaller signal in our simulations, as the investigated convective clouds are shallower and do not produce spatially extensive anvil clouds. In particular, in the context of numerical weather prediction, but also for deriving observational constraints on the cloud microphysical parameterisations, it is important to understand how these sensitivities compare to uncertainty in modelled cloud field properties due to other factors such as initial condition uncertainty or uncertainties in the formulation of other model components. To provide some context for the sensitivities discussed here, we compare them in the next section with the spread of a 10-member high-resolution initial condition ensemble.

200 4 Comparison to sensitivity to initial condition perturbations

The representation of ice formation has a fairly strong impact on the cloud microphysical properties of clouds and can induce changes of between 5 – 20 % in cloud field properties, such as accumulated precipitation, cloud fraction, and outgoing radiation fluxes (see section 3, summarised in Table. 1). In order to judge the significance of these variations, it is necessary to put them into the context of other uncertainty sources for the modelled cloud properties. As forecasts of convective situations often have a low intrinsic predictability (e.g. Hohenegger and Schär, 2007), it is particularly interesting to use ensemble simulations with perturbed initial conditions as context for sensitivity experiments regarding the model formulation. Here, we use high-resolution ensemble simulations for the COPE case, which were already used by Miltenberger et al. (2018b) to provide context for sensitivity experiments regarding the background aerosol concentration. We focus here on comparing the spread of variables between the ensemble members to the spread between different sensitivity runs. The spread from ensemble runs is indicated in all figures by the grey shaded area.

210 Altering the representation of ice formation impacts the hydrometeor number, particularly that of ice crystals (ICNC) and cloud droplets (CDNC) in the upper layers (above $\gtrsim 4.5\text{ km}$ and $\gtrsim 3\text{ km}$, respectively). These changes are much larger than the maximum spread in mean hydrometeor number profiles from the ensemble (Fig. 1 a and c). In contrast, the sensitivity of rain and graupel number densities to different ice formation representations (FSENS) is comparable to the sensitivity of the modelled clouds to perturbations in the initial conditions (Fig. 1 b and e). For snow, changes in number concentration across FSENS experiments are clearly smaller than the impact of perturbed initial conditions. Regarding the impact of secondary ice formation, here in the form of the Hallett-Mossop process, it is intriguing to note that the NoHM experiments yield mean hydrometeor profiles that are clearly outside of the ensemble spread for all frozen hydrometeor species.

220 In general the picture is very similar when hydrometeor mass mixing ratios are considered instead of their number densities (Fig. 2). The sensitivity to the ice formation representation is larger than the initial condition ensemble spread for upper-level cloud droplet and ice crystal content as well as additionally the rain water content. The NoHM experiments again have profiles outside the range from the ensemble for all hydrometeor species, but with a smaller separation from the ensemble for snow and graupel compared to the number concentration profiles (Fig. 2 d and e). Overall it appears that the sensitivity to ice formation



representation is larger than that of initial conditions perturbations even for the mean hydrometeor profiles.

225 If instead of the cloud microphysical structure the properties of the cloud field are considered the picture changes: Considering, for example, the accumulated surface precipitation the differences between FSENS and NoHM experiments is only very small if compared to the spread between members in the initial condition ensemble (Fig. 3 a). The ratio between the spread from the sensitivity experiments (FSENS & NoHM) to the spread of the ensemble is roughly 0.2. Even the difference between the baseline and the WARM experiments is much smaller than the ensemble spread. Not surprisingly, also the differences in the
230 condensate budget are much larger across the initial condition ensemble compared to the sensitivity experiments (Fig. 4 b). However, if precipitation efficiency is considered the variability across ensemble members (0.176 – 0.256) and sensitivity experiments (0.180 – 0.230) is again very similar (not shown). This suggests that the dominance of initial condition uncertainty for the accumulated precipitation is due to the strong control of larger-scale moisture and moist static energy convergence. For the conversion of this condensate to precipitation, however, the representation of cloud microphysical processes is at least as
235 important as the larger-scale meteorological conditions. In the investigated case, variability in condensate generation clearly exceeds the impact of the variability in precipitation efficiency and hence the former dominates the predicted spread of accumulated precipitation.

Similar to accumulated precipitation, also for condensed water path, cloud fraction as well as short- and long-wave outgoing radiation the spread between ensemble members is much larger than their sensitivity to a particular representation of ice formation (Fig. 5 & 6, spread ratios: 0.18, 0.047, 0.12, and 0.078, respectively). The spread between various sensitivity experiments
240 and ensemble members is summarised in Table 1.

Our analysis suggests that, at least for the investigated case forecast uncertainty is dominated by initial condition uncertainty for all cloud field variables, while uncertainty intrinsic to the representation of ice formation (reflected by parameterisation choice) place only for the detailed cloud microphysical structure a dominant role.

245 5 Discussion and Conclusions

We investigate the sensitivity of model predictions of a moderately deep convective cloud field to altered representations of ice formation (different heterogeneous freezing parameterisations, representation of Hallet-Mossop process) and to initial condition uncertainty for lead times of up to 19 h. The investigated case was selected from those observed in the COPE campaign (e.g. Leon et al., 2016). The case was already investigated in Miltenberger et al. (2018a, b) with a focus on aerosol-cloud
250 interactions.

Altering the ice formation representation impacts the cloud microphysical structure, in particular the cloud droplet, ice crystal and graupel mass mixing ratio and number concentration, as well as cloud field properties such as surface precipitation, cloud fraction and outgoing short- and long-wave radiation. Accumulated surface precipitation varies by about 8 % (21 %) and mean cloud fraction by about 7 % (7 %) across experiments with different descriptions of ice formation (only warm-phase cloud
255 microphysics). Average outgoing short-wave radiation changes by 2.9 W m^{-2} (2.9 W m^{-2}) and outgoing long-wave radiation by 1.4 W m^{-2} (0.5 W m^{-2}) in the respective set of experiments. The sensitivity to the representation of ice formation in our



case is smaller than the sensitivity found by Hawker et al. (2020) for tropical deep convective clouds. In Hawker et al. (2020), the anvils of convective clouds contributed significantly to the overall changes in cloud fraction and outgoing radiation components. In contrast, to their case cloud in our case only reach up to a stable layer in the mid-troposphere (Miltenberger et al., 260 2018a) and no anvils are present. This likely explains the smaller sensitivity to ice formation representation.

The importance of the observed sensitivity to ice formation representation for numerical weather forecasting depends on how it compares to other sources of uncertainty for predicting the cloud field evolution, including initial condition uncertainty and parametric or systematic uncertainty in other model components. In the present work, we use a high-resolution initial condition ensemble to provide context for the sensitivity experiments. From comparing the ensemble spread to the differences 265 between sensitivity experiments it becomes clear that for bulk cloud field properties such as accumulated precipitation, cloud fraction and outgoing radiation initial condition uncertainty clearly exceeds the sensitivity to the formulation of ice formation. However, for the mean hydrometeor profiles, in particular cloud droplet, ice crystal and graupel mass mixing ratios and number concentration, initial condition uncertainty is less important than the choice in ice formation parameterisation. The impact of the Hallett-Mossop process is particularly evident as the mean profiles in simulations without a representation of the 270 Hallett-Mossop processes are clearly outside of the ensemble spread. While this may indicate a significant role of secondary ice formation in this cloud type, the representation of secondary ice formation in clouds is itself highly uncertain and this uncertainty has not been explored here. The large impact of initial and boundary conditions on the bulk cloud field properties derives from the strong control of moisture and moist static energy convergence on these. Combined with the clearly different cloud microphysical structure of the clouds, this implies that altering the chosen ice formation parameterisations impacts the 275 pathway of precipitation formation, albeit with a small impact on the larger-scale cloud properties, i.e. suggesting the considered mixed-phase cloud systems maintains its large scale properties regardless of changes in the balance of the microphysical pathways.

It would be interesting to compare the sensitivity to ice formation parameterisation with the impact of other parametric uncertainties in the model. In a previous study, we have investigated the sensitivity of the same case to alterations of the aerosol 280 background concentration (factor 10 increase and decreases, respectively) (Miltenberger et al., 2018a, b). We found that the cloud field is also less sensitive to changes in aerosol conditions than to perturbations of initial conditions, at least if larger-scale properties such as accumulated precipitation, cloud fraction and radiative fluxes are considered. In sum, this suggests that COPE-type clouds are strongly controlled by meteorological conditions with comparatively little leeway for cloud microphysics to modify cloud field properties.

285 Of course the question arises, whether this dominance of initial condition uncertainty is a special feature of the chosen case. To date only few studies combine an ensemble approach with sensitivity experiments (e.g. Seifert et al., 2012) and most of these focus on idealised cases (e.g. Grabowski et al., 1999; Morrison, 2012; Wang et al., 2012; Posselt et al., 2019; Wellmann et al., 2019). Nevertheless, the overall findings are compatible with the present study, in that bulk properties such as radiative fluxes and accumulated precipitation, are strongly influenced by larger-scale meteorological conditions and to a lesser degree 290 by perturbations to the cloud microphysical scheme, be it perturbations to the aerosol environment (e.g. Seifert et al., 2012; Grabowski et al., 1999; Morrison, 2012) or to the formulation of cloud microphysical processes (e.g. Wang et al., 2012; Posselt



et al., 2019; Wellmann et al., 2019). Recently, several studies ventured to systematically investigate the joint impact of multiple uncertain parameters in the cloud microphysics representation, although again these studies have been largely focussed on idealised case (e.g. Johnson et al., 2015; Glassmeier et al., 2019). For idealised simulations of deep convection, Johnson et al. (2015) found a small impact of parameters in the immersion freezing parameterisation on accumulated precipitation compared to the impact of other parameters in the cloud microphysical parameterisation, such as collection efficiencies and aerosol number concentration, which is consistent with our COPE studies.

In summary, the simulations show that differences in ice formation parameterisation primarily impact the cloud microphysical structure with less impact on cloud field properties. Although broadly consistent with previous work, the study presented here has some shortcomings, which we plan to address in future work. Mainly it would be desirable to repeat the full ensemble simulations with the changes to the cloud microphysics representation, to investigate number of joint parameter perturbations, to test the sensitivity to the choice of the domain (e.g. White et al., 2018), and to repeat the analysis for different cases.

Data availability. Model data is stored on the tape archive provided by JASMIN (<http://www.jasmin.ac.uk/>) service. Data access to Met Office data via JASMIN is described at <http://www.ceda.ac.uk/blog/access-to-the-met-office-mass-archive-on-jasmin-goes-live/>. The data can be made accessible upon request to the authors.

Author contributions. All authors contributed to the development of the concepts and ideas presented in this paper. A. K. Miltenberger set up and run the model simulations. She also performed the model analysis and wrote the majority of the manuscript, along with input and comments from P. R. Field.

Competing interests. The authors declare that they have no conflict of interest.

310 *Disclaimer.* TEXT

Acknowledgements. We thank Adrian Hill, Ben Shipway and Jonathan Wilkinson for the development of the CASIM module. We acknowledge use of the Monsoon/NEXCS system, a collaborative facility supplied under the Joint Weather and Climate Research Programme, a strategic partnership between the Met Office and the Natural Environment Research Council. Further, we acknowledge JASMIN storage facilities (doi : 10.1109/BigData.2013.6691556). The University of Leeds and Johannes Gutenberg University Mainz are acknowledged for providing funds for this study.



References

- Atkinson, J. D., Murray, B. J., Woodhouse, M. T., Whale, T. F., Baustian, K. J., Carslaw, K. S., Dobbie, S., O'Sullivan, D., and Malkin, T. L.: The importance of feldspar for ice nucleation by mineral dust in mixed-phase clouds, *Nature*, 498, 355–358, <https://doi.org/doi:10.1038/nature12278>, 2013.
- 320 Barstad, I., Grabowski, W. W., and Smolarkiewicz, P. K.: Characteristics of large-scale orographic precipitation: Evaluation of linear model in idealized problems, *J. Hydrol.*, 340, 78–90, 2007.
- Blyth, A. M., Bennett, L. J., and Collier, C. G.: High-resolution observations of precipitation from cumulonimbus clouds, *Meteorol. Appl.*, 22, 75–89, <https://doi.org/10.1002/met.1492>, 2015.
- Bowler, N. E., Arribas, A., Mylne, K. R., Robertson, K. B., and Beare, S. E.: The MOGREPS short-range ensemble prediction system, *Q. J. R. Meteorol. Soc.*, 134, 703–722, <https://doi.org/10.1002/qj.234>, 2008.
- 325 Cooper, W. A.: Ice Initiation in Natural Clouds, pp. 29–32, American Meteorological Society, Boston, MA, https://doi.org/10.1007/978-1-935704-17-1_4, 1986.
- DeMott, P. J., Prenni, A. J., Liu, X., Kreidenweis, S. M., Petters, M. D., Twohy, C. H., Richardson, M. S., Eidhammer, T., and Rogers, D. C.: Predicting global atmospheric ice nuclei distributions and their impacts on climate, *Proc. Natl. Acad. Sci. USA*, 107, 11 217–11 222, <https://doi.org/10.1073/pnas.0910818107>, 2010.
- 330 DeMott, P. J., Prenni, A. J., McMeeking, G. R., Sullivan, R. C., Petters, M. D., Tobo, Y., Niemand, M., Möhler, O., Snider, J. R., Wang, Z., and Kreidenweis, S. M.: Integrating laboratory and field data to quantify the immersion freezing ice nucleation activity of mineral dust particles, *Atmos. Chem. Phys.*, 15, 393–409, <https://doi.org/10.5194/acp-15-393-2015>, 2015.
- Dey, S. R. A., Leoncini, G., Roberts, N. M., Plant, R. S., and Migliorini, S.: A spatial view of ensemble spread in convection permitting ensembles, *Mon. Wea. Rev.*, 142, 4091–4107, <https://doi.org/10.1175/MWR-D-14-00172.1>, 2014.
- 335 Field, P. R. and Heymsfield, A. J.: Importance of snow to global precipitation, *Geophys. Res. Lett.*, 42, 9512–9520, <https://doi.org/10.1002/2015GL065497>, 2015.
- Field, P. R., Lawson, R. P., Brown, P. R. A., Lloyd, G., Westbrook, C., Moisseev, D., Miltenberger, A., Nenes, A., Blyth, A., Choulaton, T., Connolly, P., Buehl, J., Crosier, J., Cui, Z., Dearden, C., DeMott, P., Flossmann, A., Heymsfield, A., Huang, Y., Kalesse, H., Kanji, Z. A., Korolev, A., Kirchgaessner, A., Lasher-Trapp, S., Leisner, T., McFarquhar, G., Phillips, V., Stith, J., and Sullivan, S.: Secondary Ice Production: Current State of the Science and Recommendations for the Future, *Meteorol. Monographs*, 58, 7.1–7.20, <https://doi.org/10.1175/AMSMONOGRAPHS-D-16-0014.1>, 2017.
- 340 Glassmeier, F., Hoffmann, F., Johnson, J. S., Yamaguchi, T., Carslaw, K. S., and Feingold, G.: An emulator approach to stratocumulus susceptibility, *Atmos. Chem. Phys.*, 19, 10 191–10 203, <https://doi.org/10.5194/acp-19-10191-2019>, 2019.
- 345 Grabowski, W. W., Wu, X., and Moncrieff, M. W.: Cloud Resolving Modeling of Tropical Cloud Systems during Phase III of GATE. Part III: Effects of Cloud Microphysics, *J. Atmos. Sci.*, 56, 2384–2402, [https://doi.org/10.1175/1520-0469\(1999\)056<2384:CRMOTC>2.0.CO;2](https://doi.org/10.1175/1520-0469(1999)056<2384:CRMOTC>2.0.CO;2), 1999.
- Hawker, R., Miltenberger, A. K., Wilkinson, J. M., Hill, A. A., Shipway, B. J., Cui, Z., Cotton, R. J., Carslaw, K. S., Field, P. R., and Murray, B. J.: The nature of ice-nucleating particles affects the radiative properties of tropical convective cloud systems, *Atmos. Chem. Phys. Diss.*, submitted manuscript number acp-2020-571, 2020.
- 350 Hohenegger, C. and Schär, C.: Predictability and error growth dynamics in cloud-resolving models, *J. Atmos. Sci.*, 64, 4467–4478, <https://doi.org/10.1175/2007JAS2143.1>, 2007.



- Johnson, J. S., Cui, Z., Lee, L. A., Gosling, J. P., Blyth, A. M., and Carslaw, K. S.: Evaluating uncertainty in convective cloud microphysics using statistical emulation, *J. Adv. Model. Earth Syst.*, 7, 162–187, <https://doi.org/10.1002/2014MS000383>, 2015.
- 355 Khain, A. P.: Notes on state-of-the-art investigations of aerosol effects on precipitation: A critical review, *Environ. Res. Lett.*, 4, 015 004, <https://doi.org/10.1088/1748-9326/4/1/015004>, 2009.
- Klein, S. A., McCoy, R. B., Morrison, H., Ackerman, A. S., Avramov, A., Boer, G. d., Chen, M., Cole, J. N. S., Del Genio, A. D., Falk, M., Foster, M. J., Fridlind, A., Golaz, J.-C., Hashino, T., Harrington, J. Y., Hoose, C., Khairoutdinov, M. F., Larson, V. E., Liu, X., Luo, Y., McFarquhar, G. M., Menon, S., Neggers, R. A. J., Park, S., Poellot, M. R., Schmidt, J. M., Sednev, I., Shipway, B. J., Shupe, M. D.,
360 Spangenberg, D. A., Sud, Y. C., Turner, D. D., Veron, D. E., Salzen, K. v., Walker, G. K., Wang, Z., Wolf, A. B., Xie, S., Xu, K.-M., Yang, E., and Zhang, G.: Intercomparison of model simulations of mixed-phase clouds observed during the ARM Mixed-Phase Arctic Cloud Experiment. I: single-layer cloud, *Q. J. R. Meteorol. Soc.*, 135, 979–1002, <https://doi.org/10.1002/qj.416>, 2009.
- Korolev, A., McFarquhar, G., Field, P. R., Franklin, C., Lawson, P., Wang, Z., Williams, E., Abel, S. J., Axisa, D., Borrmann, S., Crosier, J., Fugal, J., Krämer, M., Lohmann, U., Schlenker, O., Schnaiter, M., and Wendisch, M.: Mixed-phase clouds: Progress and challenges,
365 *Meteorol. Monographs*, 58, 5.1–5.50, <https://doi.org/10.1175/AMSMONOGRAPHIS-D-17-0001.1>, 2017.
- Leon, D. C., French, J. R., Lasher-Trapp, S., Blyth, A. M., Abel, S. J., Ballard, S., Barrett, A., Bennett, L. J., Bower, K., Brooks, B., Brown, P., Charlton-Perez, C., Choulaton, T., Clark, P., Collier, C., Crosier, J., Cui, Z., Dey, S., Dufton, D., Eagle, C., Flynn, M. J., Gallagher, M., Halliwell, C., Hanley, K., Hawkness-Smith, L., Huang, Y., Kelly, G., Kitchen, M., Korolev, A., Lean, H., Liu, Z., Marsham, J., Moser, D., Nicol, J., Norton, E. G., Plummer, D., Price, J., Ricketts, H., Roberts, N., Rosenberg, P. D., Simonin, D., Taylor, J. W., Warren, R.,
370 Williams, P. I., and Young, G.: The Convective Precipitation Experiment (COPE): Investigating the origins of heavy precipitation in the Southwestern United Kingdom, *Bull. Am. Meteor. Soc.*, 97, 1003–1020, <https://doi.org/10.1175/BAMS-D-14-00157.1>, 2016.
- Levin, Z., Teller, A., Ganor, E., and Yin, Y.: On the interactions of mineral dust, sea-salt particles, and clouds: A measurement and modeling study from the Mediterranean Israeli Dust Experiment campaign, *J. Geophys. Res. Atmos.*, 110, <https://doi.org/10.1029/2005JD005810>, 2005.
- 375 Lohmann, U. and Hoose, C.: Sensitivity studies of different aerosol indirect effects in mixed-phase clouds, *Atmos. Chem. Phys.*, 9, 8917–8934, <https://doi.org/10.5194/acp-9-8917-2009>, 2009.
- McCoy, D. T., Tan, I., Hartmann, D. L., Zelinka, M. D., and Storelvmo, T.: On the relationships among cloud cover, mixed-phase partitioning, and planetary albedo in GCMs, *J. Adv. Model. Earth Systems*, 8, 650–668, <https://doi.org/10.1002/2015MS000589>, 2016.
- Meyers, M. P., DeMott, P. J., and Cotton, W. R.: New primary ice-nucleation parameterizations in an explicit cloud model, *J. Appl. Meteor.*,
380 31, 708–721, 1992.
- Miltenberger, A. K.: Lagrangian perspective on dynamic and microphysical processes in orographically forced flows, Ph.D. thesis, ETH Zurich, <https://doi.org/10.3929/ethz-a-010406950>, 2014.
- Miltenberger, A. K., Field, P. R., Hill, A. A., Rosenberg, P., Shipway, B. J., Wilkinson, J. M., Scovell, R., and Blyth, A. M.: Aerosol–cloud interactions in mixed-phase convective clouds – Part 1: Aerosol perturbations, *Atmos. Chem. Phys.*, 18, 3119–3145,
385 <https://doi.org/10.5194/acp-18-3119-2018>, 2018a.
- Miltenberger, A. K., Field, P. R., Hill, A. A., Shipway, B. J., and Wilkinson, J. M.: Aerosol–cloud interactions in mixed-phase convective clouds – Part 2: Meteorological ensemble, *Atmos. Chem. Phys.*, 18, 10 593–10 613, <https://doi.org/10.5194/acp-18-10593-2018>, 2018b.
- Morrison, H.: On the robustness of aerosol effects on an idealized supercell storm simulated with a cloud system-resolving model, *Atmos. Chem. Phys.*, 12, 7689–7705, 2012.



- 390 Niemand, M., Möhler, O., Vogel, B., Vogel, H., Hoose, C., Connolly, P., Klein, H., Bingemer, H., DeMott, P., Skrotzki, J., and Leisner, T.: A particle-surface-area-based parameterization of immersion freezing on desert dust particles, *J. Atmos. Sci.*, **69**, 3077–3092, <https://doi.org/10.1175/JAS-D-11-0249.1>, 2012.
- Posselt, D. J., He, F., Bukowski, J., and Reid, J. S.: On the Relative Sensitivity of a Tropical Deep Convective Storm to Changes in Environment and Cloud Microphysical Parameters, *J. Atmos. Sci.*, **76**, 1163–1185, <https://doi.org/10.1175/JAS-D-18-0181.1>, 2019.
- 395 Seifert, A., Köhler, C., and Beheng, K. D.: Aerosol-cloud-precipitation effects over Germany as simulated by a convective-scale numerical weather prediction model, *Atmos. Chem. Phys.*, **12**, 709–725, 2012.
- Sullivan, S. C., Hoose, C., Kiselev, A., Leisner, T., and Nenes, A.: Initiation of secondary ice production in clouds, *Atmos. Chem. Phys.*, **18**, 1593–1610, <https://doi.org/10.5194/acp-18-1593-2018>, 2018.
- Tobo, Y., Prenni, A. J., DeMott, P. J., Huffman, J. A., McCluskey, C. S., Tian, G., Pöhlker, C., Pöschl, U., and Kreidenweis, S. M.: Biological aerosol particles as a key determinant of ice nuclei populations in a forest ecosystem, *J. Geophys. Res.*, **118**, 10 100–10 110, <https://doi.org/10.1002/jgrd.50801>, 2013.
- 400 Vergara-Temprado, J., Miltenberger, A. K., Furtado, K., Grosvenor, D. P., Shipway, B. J., Hill, A. A., Wilkinson, J. M., Field, P. R., Murray, B. J., and Carslaw, K. S.: Strong control of Southern Ocean cloud reflectivity by ice-nucleating particles, *Proc. Natl. Acad. Sci. USA*, **115**, 2687–2692, <https://doi.org/10.1073/pnas.1721627115>, 2018.
- 405 Wang, H., Auligné, T., and Morrison, H.: Impact of Microphysics Scheme Complexity on the Propagation of Initial Perturbations, *Mon. Wea. Rev.*, **140**, 2287–2296, <https://doi.org/10.1175/MWR-D-12-00005.1>, 2012.
- Wellmann, C., Barrett, A. I., Johnson, J. S., Kunz, M., Vogel, B., Carslaw, K. S., and Hoose, C.: Comparing the impact of environmental conditions and microphysics on the forecast uncertainty of deep convective clouds and hail, *Atmos. Chem. Phys.*, 2019, 1–26, <https://doi.org/10.5194/acp-2019-558>, 2019.
- 410 White, B. A., Buchanan, A. M., Birch, C. E., Stier, P., and Pearson, K. J.: Quantifying the Effects of Horizontal Grid Length and Parameterized Convection on the Degree of Convective Organization Using a Metric of the Potential for Convective Interaction, *J. Atmos. Sci.*, **75**, 425–450, <https://doi.org/10.1175/JAS-D-16-0307.1>, 2018.
- Wilson, T. W., Ladino, L. A., Alpert, P. A., Breckels, M. N., Brooks, I. M., Browse, J., Burrows, S. M., Carslaw, K. S., Huffman, J. A., Judd, C., Kilhau, W. P., Mason, R. H., McFiggans, G., Miller, L. A., Nájera, J. J., Polishchuk, E., Rae, S., Schiller, C. L., Si, M., Temprado, J. V., Whale, T. F., Wong, J. P. S., Wurl, O., Yakobi-Hancock, J. D., Abbatt, J. P. D., Aller, J. Y., Bertram, A. K., Knopf, D. A., and Murray, B. J.: A marine biogenic source of atmospheric ice-nucleating particles, *Nature*, **525**, 234–238, <https://doi.org/10.1038/nature14986>, 2015.



Table 1. Maximum difference between mean cloud droplet number concentration (CDNC), ice crystal number concentration (ICNC), cloud mass mixing ratio (q_c), frozen hydrometeor mass mixing ratio (q_f), accumulated surface precipitation (P), condensed water path (TWP), cloud fraction, and outgoing short-wave (OSR) as well as long-wave (OSR) radiation.

Variable	ensemble (max-min)	FSENS (max-min)	FSENS, DM10 (max-min)	baseline - NoHM	baseline - WARM
$\log_{10}(\text{CDNC}) (> 4.5 \text{ km})$	0.751	0.987	0.266	-0.118	-1.22
$\log_{10}(\text{ICNC}) (> 4.5 \text{ km})$	0.421	1.02	0.519	0.307	-
$\log_{10}(\text{ICNC}) (< 4.5 \text{ km})$	0.280	0.619	0.155	1.05	-
$\log_{10}(q_c) (> 4.5 \text{ km})$	0.979	1.04	0.486	-0.377	-1.29
$\log_{10}(q_f) (> 4.5 \text{ km})$	0.424	0.244	0.120	0.325	-
$\log_{10}(q_f) (< 4.5 \text{ km})$	0.258	0.126	0.106	0.279	-
P [10^9 kg]	20.0	2.71	0.863	-2.02	7.12
TWP [kg m^{-2}]	5.17	0.861	0.543	0.463	1.15
cloud fraction	0.159	$0.842 \cdot 10^{-2}$	$0.506 \cdot 10^{-2}$	$0.255 \cdot 10^{-2}$	$0.420 \cdot 10^{-2}$
OSR [W m^{-2}]	23.0	2.89	1.46	1.79	-4.87
OLR [W m^{-2}]	3.75	0.270	0.139	0.143	0.487

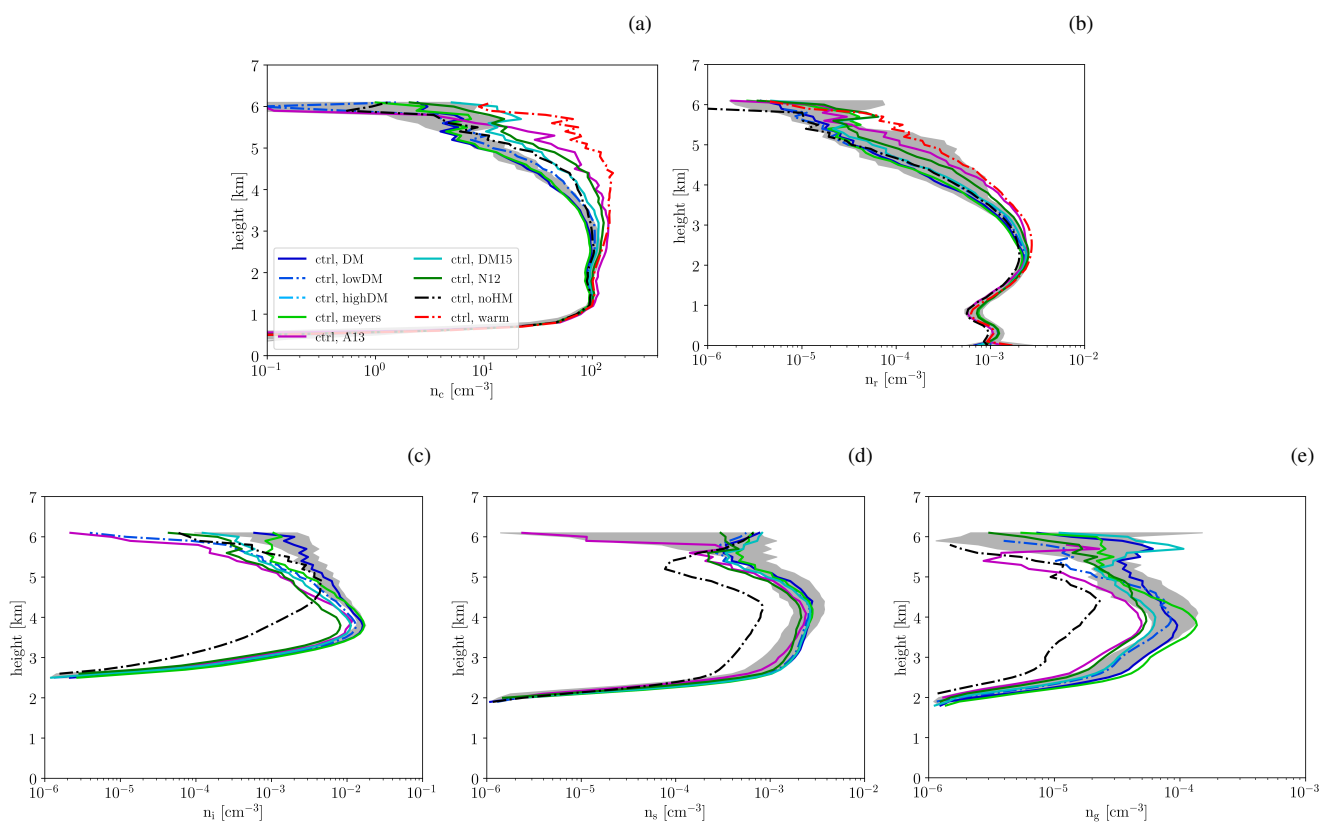


Figure 1. Average profiles of in-cloud number concentrations of (a) cloud droplets, (b) rain drops, (c) ice crystals, (d) snow and (e) graupel. Different coloured lines show the profiles from simulations with different heterogeneous freezing parameterisations, different INP number concentrations, without a parameterisation of the Hallett-Mossop process and with warm cloud microphysics only (colours according to legend). The grey shading shows the spread of the average profiles in the 10-member high-resolution ensemble with the DeMott et al. (2010) heterogeneous freezing parameterisation and a representation of the Hallett-Mossop process. The 0 °C level is located at about 2.6 km altitude.

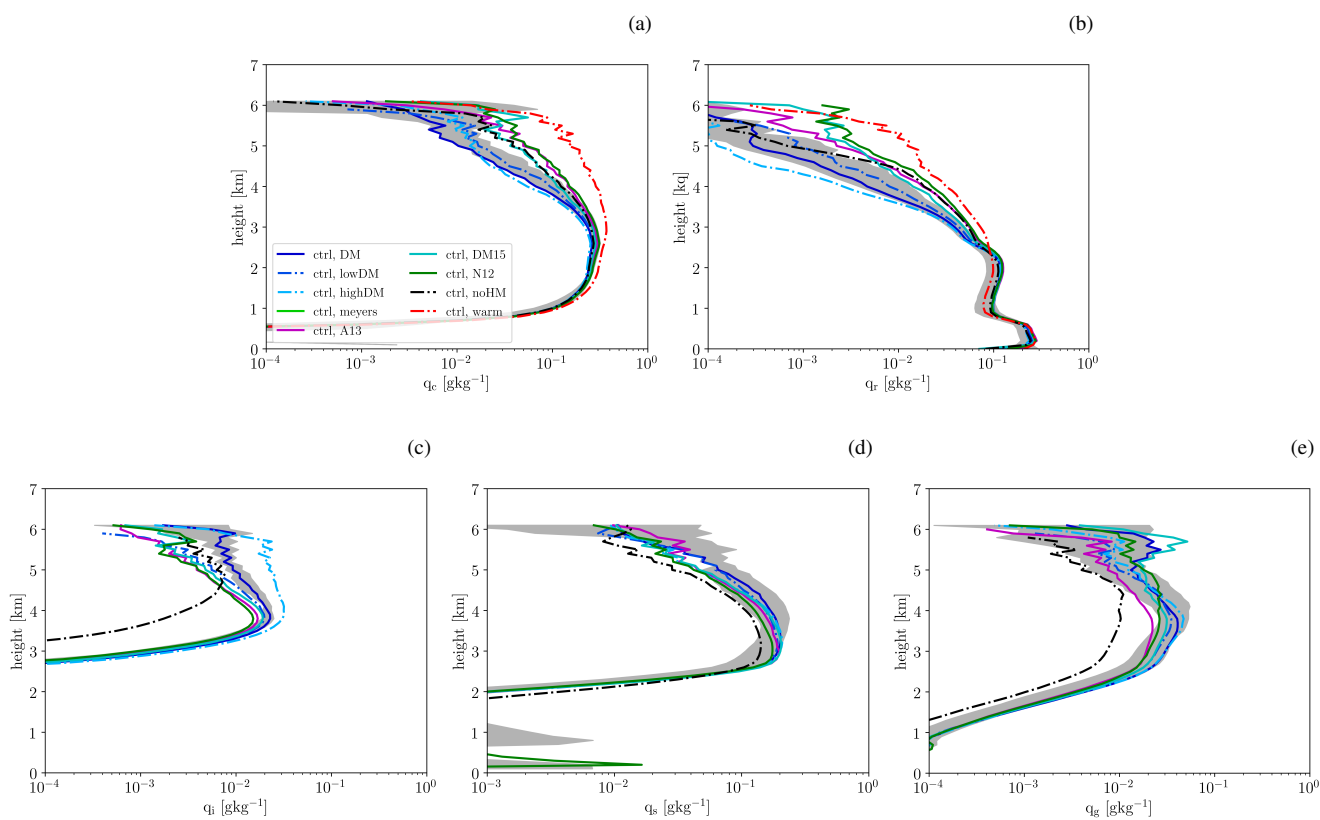


Figure 2. Same as Fig. 1 but for hydrometeor mass mixing ratios.

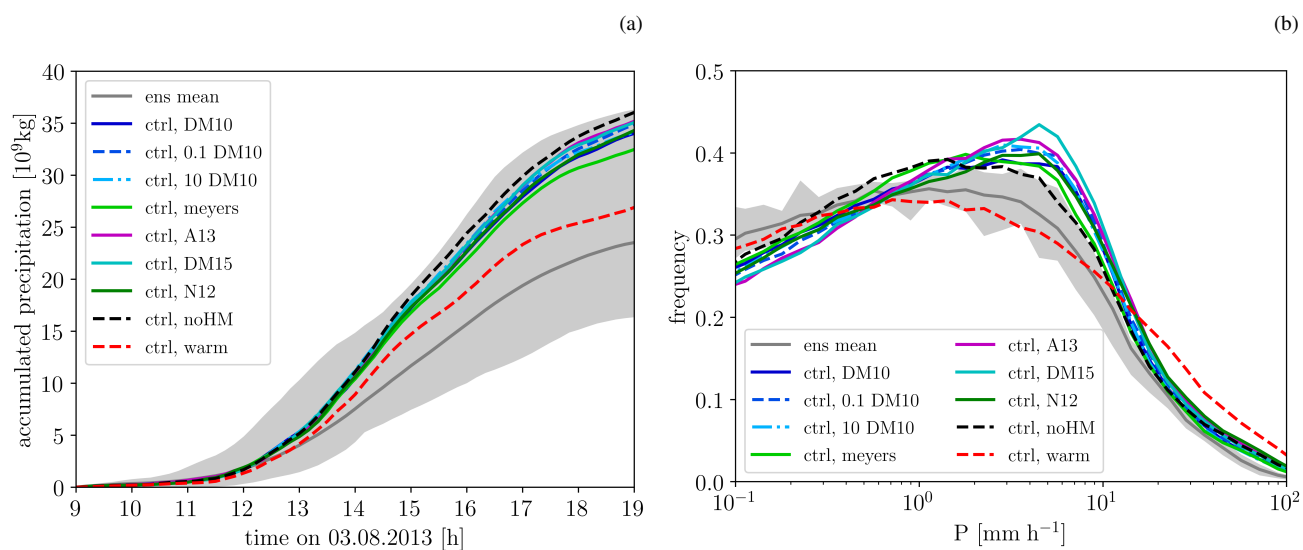


Figure 3. (a) Time series of accumulated surface precipitation. (b) Precipitation rate distribution (excluding non-raining grid-points). The dark grey shading shows the spread of the 10 ensemble members with perturbed initial conditions. The grey line represents the ensemble mean and the various coloured lines simulations with different heterogeneous freezing parameterisation, pure warm-phase microphysics and no Hallett-Mossop process (colours according to legend).

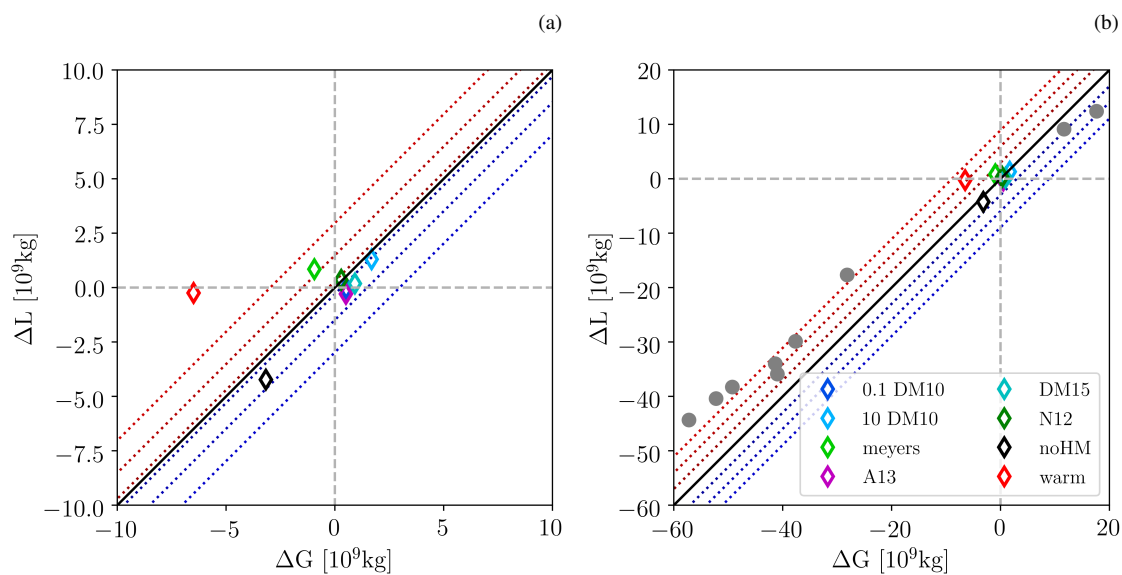


Figure 4. Scatterplot of change in condensate gain ΔG and condensate loss ΔL relative to the simulation with the DeMott et al. (2010) heterogeneous freezing parameterisation and a representation of the Hallett-Mossop process (baseline simulation). The condensate gain in the baseline simulation is $137.0 \cdot 10^9 \text{ kg}$ and the condensate loss $107.3 \cdot 10^9 \text{ kg}$. The grey symbols in panel (b) represent the 9 meteorological ensemble members other than the baseline simulation. The blue and red dashed lines indicate relative changes in precipitation of 0.1, 5, 10 % in (a) and 10, 20, 30 % in (b).

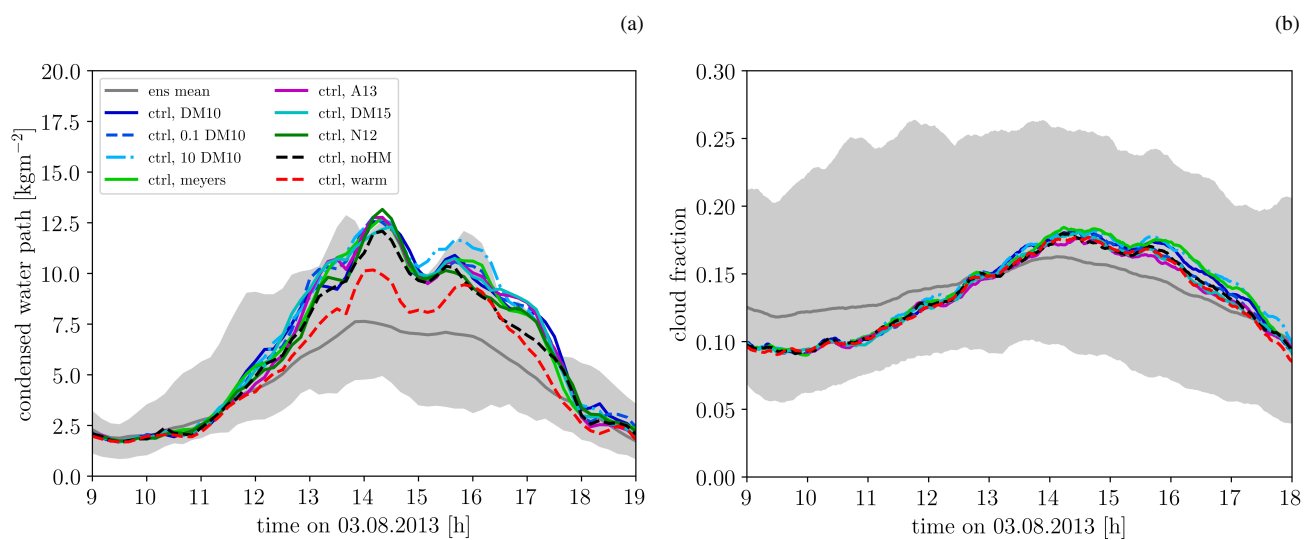


Figure 5. Time series of (a) the average condensed water path and (b) the cloud fraction. The dark grey shading in both panels shows the spread of the 10 ensemble members with perturbed initial conditions. The grey line represents the ensemble mean and the various coloured lines simulations with different heterogeneous freezing parameterisation, pure warm-phase microphysics and no Hallett-Mossop process (colours according to legend).

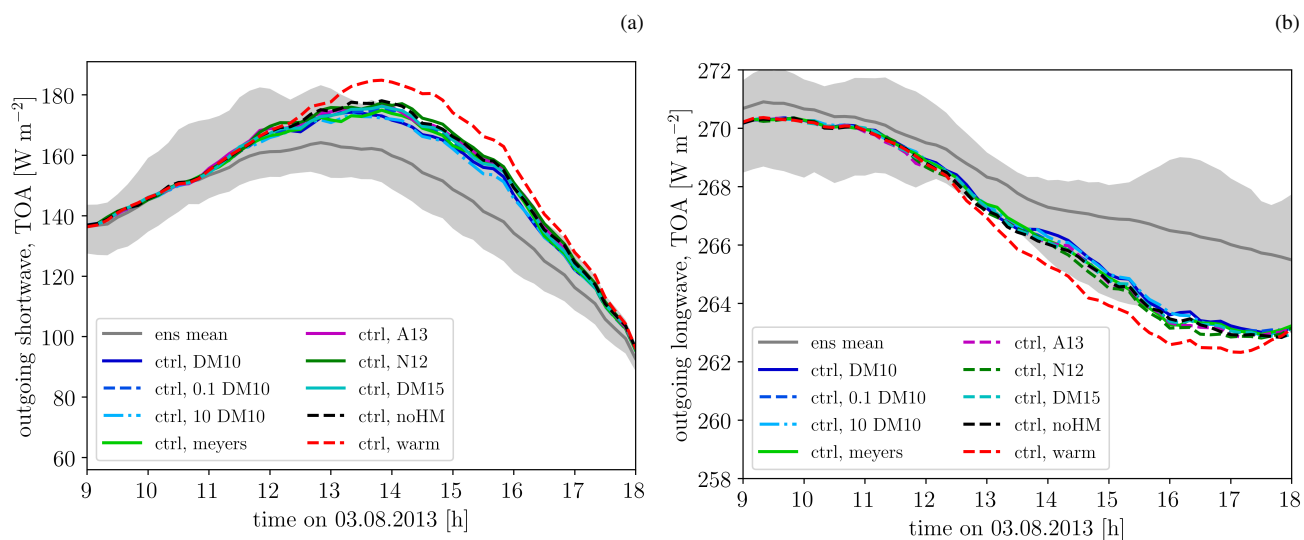


Figure 6. Domain-average time series of outgoing (a) shortwave and (b) longwave radiation at the top of atmosphere. The dark grey shading shows the spread of the 10 ensemble members with perturbed initial conditions. The grey line represents the ensemble mean and the various coloured lines simulations with different heterogeneous freezing parameterisation, pure warm-phase microphysics and no Hallett-Mossop process.